Conformational independence of N- and C-domains in ribosomal protein L7/L12 and in the complex with protein L10

E.V. Bocharov[a], A.T. Gudkov[b], E.V. Budovskaya[b], A.S. Arseniev[a,*]

[a] *Shemyakin–Ovchinnikov Institute of Bioorganic Chemistry, Russian Academy of Sciences, ul. Miklukho-Maklaya, 16/10, Moscow 117871, Russia*
[b] *Institute of Protein Research, Russian Academy of Sciences, Pushchino, Moscow Region, Russia*

Received 24 December 1997; revised version received 23 January 1998

Abstract Isolated N- (1–37) and C-terminal (47–120) fragments of L7 protein, and pentameric $(L7)_4L10$ complex were studied by NMR spectroscopy in solution. The results indicate that the dimer state of the 1–37 fragment with a helical hairpin conformation is identical to the N-terminal structure of the intact L7 dimer. The C-terminal domain of the L7 protein does not participate in $(L7)_4L10$ complex formation. The overall motions of the L7 C-domains are essentially independent both in the L7 dimer and in the $(L7)_4L10$ complex. Conformational motions on a millisecond time scale are detected in the $(L7)_4L10$ complex. The possible relevance of these motions to the biological function of L7/L12 is discussed.

Key words: Ribosome; L7/L12 protein; L10 protein; L7-L10 complex; Nuclear magnetic resonance; Structure

1. Introduction

The L7/L12 protein of *Escherichia coli* is one of the most thoroughly investigated ribosomal proteins (for a review see [1]). L7/L12 consists of 120 amino acid residues and L7 is the N-terminal acetylated form of L12. It is known that L7/L12 is important for the functioning of the elongation factors involved in ribosomal protein synthesis. In solution the L7/L12 protein exists as a dimer; two dimers are associated with other ribosomal components via L10 protein.

Spatial structures of the C-terminal fragment and intact L7/L12 were studied by X-ray crystallography [2] and NMR spectroscopy [3], respectively. As a result the following model of the L7/L12 dimer was derived [3]: two N-terminal parts (residues 1–33) form a four-helical bundle and two globular C-terminal domains (residues 51–120) are connected to the bundle via highly mobile hinge regions. The N-terminal part of the L7/L12 dimer is responsible for its incorporation into the ribosome [4,5]. According to ^{1}H-NMR data [6], the L7/L12 C-domains have large mobility in the ribosome. The results of fluorescence polarization measurements [7,8] suggest that in the L7/L12 dimer the C-domains are separated and their motion is diminished when the hinge region is shortened. The length of the flexible hinge region, but not its amino acids composition, is crucial for the function of the L7/L12 dimer in the ribosomes. Deletion of residues 44–52 or 38–52 in L7/L12 produces virtually inactive ribosomes, while the mutant with 14 added residues in the hinge region is functionally active [9].

Hence, the mobility of L7/L12 is relevant for the functioning of this protein during the translation process. To establish the conformational behavior of the L7/L12 domains, we studied the N- and C-terminal fragments of the L7/L12 protein and tight complex between the L10 and L7/L12 proteins [10] by heteronuclear NMR spectroscopy.

2. Materials and methods

The 1–37 fragment and uniformly ^{15}N-labeled L7 protein were obtained according to procedures described in [4] and [3,11], respectively.

The uniformly ^{15}N-labeled C-terminal fragment (residues 47–120) was obtained after spontaneous proteolysis in the flexible hinge region of the L7 dimer [12]. The degraded sample (spontaneous proteolysis throughout 3 weeks) of the ^{15}N-labeled L7 dimer contained two fragments of about 4 kDa and 7.5 kDa. The C-terminal fragment was separated from the mixture on a Sephadex G-50 column with 6 M urea.

To form the $(L7)_4L10$ complex the L10 protein obtained as described previously [10] and an excess of ^{15}N-labeled L7 were dissolved in 2 M guanidinium chloride. The $(L7)_4L10$ complex was isolated on a G-100 Sephadex column equilibrated with 10 mM ammonium acetate buffer, pH 7.8.

Due to the instability of the 1–37 fragment in solution, only 2D TOCSY (40 ms) [13] and 2D NOESY (200 ms) [14] spectra were acquired satisfactorily. Resonance assignments of the 1–37 fragment were obtained using a standard procedure [15]. The 2D NOESY experiment for the $(L7)_4L10$ complex was performed with a mixing period of 100 ms. The water signal was suppressed by the jump-and-return (jr) technique accompanied by a weak presaturation pulse (field strength 25 Hz) during the relaxation delay.

Heteronuclear 2D ^{1}H-^{15}N HMQC spectra [16] of the L7 dimer, L7 C-terminal fragment and $(L7)_4L10$ complex were acquired with a weak presaturation pulse during the relaxation delay. The water flip-back gradient enhanced 2D ^{1}H-^{15}N HSQC spectrum of the L7 dimer was acquired according to [17] without water saturation. The ^{1}H-^{15}N spectra were obtained with a ^{15}N-dimension spectral width of 2000 Hz for the whole spectrum and of 1400 Hz for the wrapped up spectrum.

All NMR spectra were acquired at 30°C on a UNITY-600 Varian spectrometer. Buffer solution for the samples contained 0.05 M sodium phosphate, 0.1 M KCl and 10% D_2O+90% H_2O, pH 6.9. The NMR spectra were processed with the VNMR program, Varian software, and analyzed with the XEASY program [18]. Residual solvent signal was removed from the spectra by convolution of the time domain data during data processing. After applying Gaussian filter, zero filling, Fourier transformation and baseline correction the final complex data matrices were 2048×4096 and 1024×2048 points for proton and heteronuclear spectra, respectively.

^{1}H chemical shifts are given relative to the internal standard, sodium 2,2-dimethyl-2-silapentane sulfonate. ^{15}N chemical shifts are reported relative to the external standard containing 2.9 M $^{15}NH_4Cl$ in 1 M HCl (24.93 ppm).

The secondary structure of the L10 protein was predicted by the

*Corresponding author. Fax: (7) (95) 335-50-33.
E-mail: aars@nmr.ru

Abbreviations: 2D, two-dimensional; NOE, nuclear Overhauser enhancement; NOESY, 2D NOE-correlated spectroscopy; TOCSY, 2D total correlated spectroscopy; HSQC and HMQC, 2D ^{1}H-detected heteronuclear single and multiple quantum correlation; jr, the jump-and-return method of solvent signal suppression

PII S0014-5793(98)00121-5

WWW molecular biology server ExPASy provided by the Geneva University Hospital and the University of Geneva [19].

3. Results and discussion

3.1. 1–37 fragment of L7

The 1–37 fragment is capable of interacting with 50S subparticles like the intact L7/L12 protein [4]. Analysis of the 2D NOESY spectra revealed a specific pattern of NOE connectivities indicating the secondary structure of the 1–37 fragment. Stretches of the $d_{NN}(i,i+1)$, $d_{\alpha N}(i,i+3)$, $d_{\alpha N}(i,i+4)$ and $d_{\alpha\beta}(i,i+3)$ connectivities and secondary chemical shift indices of $C^{\alpha}H$ protons are characteristic [15,20] of two helical regions (residues Lys^{4}–Ala^{12} and Val^{19}–Gly^{31}) (Fig. 1). Using sequence-specific resonance assignments and NOEs we compared the secondary structure topology of the 1–37 fragment with that of the L7 dimer [3]. Proton chemical shifts of the 1–37 fragment are identical to those of the L7 dimer within 0.03 ppm tolerance, and the pattern of the NOE connectivities of the 1–37 fragment (Fig. 1) is similar to the one of the L7 dimer (see Fig. 2 in [3]). These data shows that the spatial structure of the 1–37 fragment is identical to that of the N-domain of the intact L7 dimer [3]. The 1–37 fragment is a symmetric dimer, comprising four antiparallel helices (2αD, residues Lys^{4}–Ala^{12}, and 2αE, residues Val^{19}–Phe^{30}).

3.2. 47–120 fragment of L7

Comparative analysis of the ^{1}H-^{15}N HMQC spectra of the 47–120 fragment and intact L7 dimer shows (see Fig. 2) that the cross-peaks from amide groups of C-terminal residues 48–120 have almost identical positioning in the spectra. The largest differences (less than 0.06 ppm) of chemical shifts of amide protons for the samples are observed for the residues Glu^{50}, Asn^{64}, Glu^{82}, Lys^{84} and Asp^{85}, which are the most sensitive to small pH changes. Thus, summarizing the findings for the

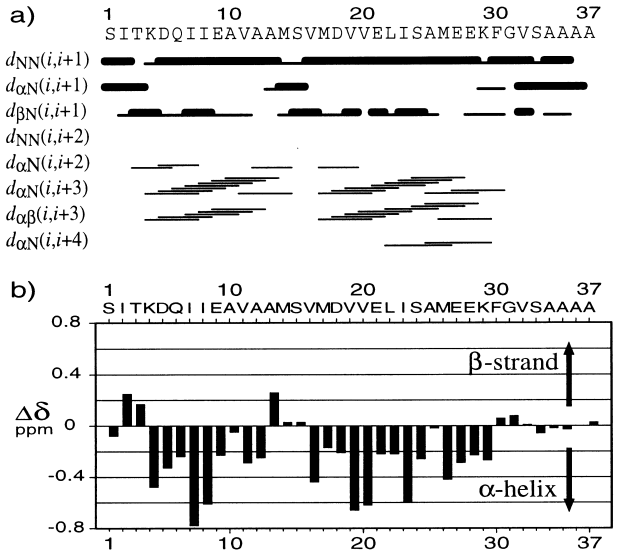

Fig. 1. Overview of NMR data defining the secondary structure of the L7 1–37 fragment. a: Summary of the sequential and medium-range NOEs. The observed NOEs classified as strong and weak are shown by thick and thin lines, respectively. b: Comparison of backbone $C^{\alpha}H$ chemical shifts of the 1–37 fragment residues (horizontal axis) with random coil values. The arrows display a tendency of α-proton secondary chemical shift, $\Delta\delta = \delta_{L7} - \delta_{random\ coil}$, for β-strand and α-helix backbone conformations of protein.

1–37 and 47–120 fragments, it can be stated that isolated N- and C-terminal fragments of L7/L12 have structures similar to those in the L7/L12 dimer.

3.3. Pentameric complex

In the NOESY spectrum of the $(L7)_4L10$ complex the cross-peaks of the L7 C-domain and some cross-peaks of L10 are distinctly detected, whereas signals of the L7 N-domain are not observed (data not shown). In spite of the high signal-to-noise ratio (approximately 150:1) for most of the cross-peaks in the HMQC spectrum of the $(L7)_4L10$ complex, no cross-peaks of the L7 N-terminal residues from Ser^{1} to Ala^{39} are observable (Fig. 2c), i.e. they are broadened beyond detection due to specific interaction with the L10 protein. From the comparison of the ^{1}H-^{15}N heteronuclear spectra of the $(L7)_4L10$ complex and L7 dimer (see Fig. 2) it can be concluded that the complex formation does not change cross-peak positions (within ±0.04 ppm tolerance for amide protons) of the Val^{40}–Lys^{120} residues. This indicates that the L7 C-domains and most of the hinge region residues are not involved in $(L7)_4L10$ complex formation and their structure remains the same as in the L7 dimer. Thus, only the L7 N-domains interact with the L10 protein. The signal broadening beyond detection in the L7 N-terminal part (residues 1–39) can be explained by conformational motions on the millisecond time scale, rather than by an increase of overall correlation time, which was evaluated to be 20–30 ns for the $(L7)_4L10$ complex using the Stokes-Einstein equation.

The minor differences of the C-domain cross-peak positions in ^{1}H-^{15}N heteronuclear spectra of the 47–120 fragment, L7 dimer and $(L7)_4L10$ complex might result from small variations of external conditions and solution composition from sample to sample, rather than from any structural difference within the L7 C-domain. The slightly increased line width in the proton direction of the HMQC spectra indicates a minor increase of the overall correlation time of the C-domains (line broadening is about 15% for the L7 dimer and about 35% for the $(L7)_4L10$ complex relative to the 47–120 fragment). Taking into account that the 47–120 fragment is monomeric in solution at millimolar concentrations [5], we conclude that the C-domains remain in the separated state most of the time both in the L7 dimer and in the $(L7)_4L10$ complex. It does not mean, however, that after interaction of L7/L12 with the translation factors the situation will be the same.

It is known [21] that the L10 C-terminal fragment (residues 71–164) can bind two L7/L12 dimers, while the L10 N-terminal fragment (1–70) is responsible for binding to 23S ribosomal RNA. Theoretical evaluations (WWW server ExPASy [19]) of L10 secondary structure show that residues 90–164 tend to attain α-helical conformation, while the sequence of the N-terminal part reveals a split β-α-β motif typical of RNA binding proteins [22,23]. Hence, it is most likely that the $(L7)_4L10$ complex is stabilized by helix-helix interaction of the L10 C-terminal part with the N-domains of two L7 dimers. This is confirmed by calorimetric and circular dichroism studies [10], which revealed that the number of residues in α-helical conformation was greater by 20–25 in the $(L7)_4L10$ complex compared to the free L7 and L10 proteins, and that the thermal stability of the L10 protein was vastly increased in the complex. Since the L7 N-domains are fully helix-laden and the dimerization state of L7 is retained in the ribosomes [4], we can conclude that the symmetrical structure of the L7 N-

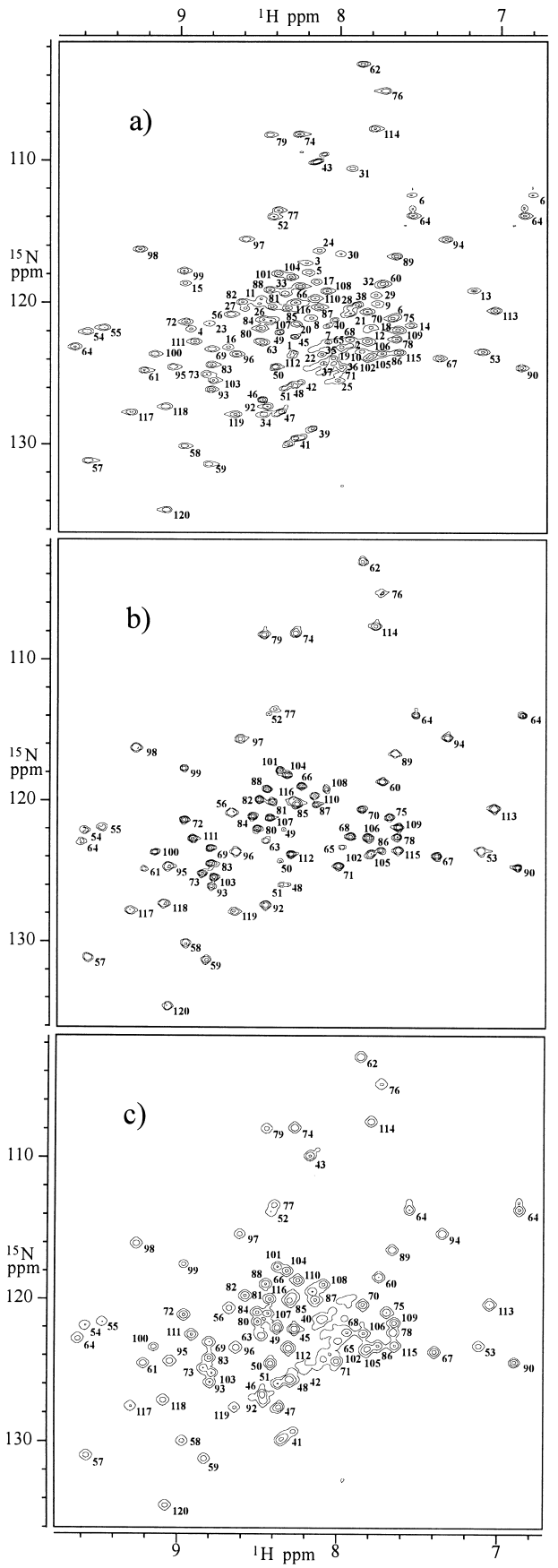

Fig. 2. ^{1}H-^{15}N HSQC (a) and HMQC spectra (b) of the uniformly ^{15}N-labeled L7 dimer and L7 47–120 fragment, respectively. c: ^{1}H-^{15}N HMQC spectrum of the pentameric $(L7)_4L10$ complex with uniformly ^{15}N-labeled L7 and unlabeled L10. The spectra were recorded at pH 6.9 and 30°C. ^{1}H-^{15}N backbone resonance assignments are indicated by numbers.
←

terminal domains is maintained or undergoes insignificant changes upon $(L7)_4L10$ complex formation.

Some general assumptions can be drawn regarding the conformational motions in the complex. The motions can be caused by exchange of the L7 dimers between two different binding sites in L10 and/or by transitions of the L7 dimers between structurally equivalent conformations (Fig. 3). We shall describe the second possibility in detail. When the symmetric N-domain of the L7 dimer with a rotary axis of second order symmetry gets into the asymmetrical spatial environment of L10, the N-domain can attain one of the two equally possible orientations, which are transferred one into the other by a 180° turn (Fig. 3). These 'flip-flop' transitions may explain the millisecond conformational motions of the L7 N-domains in the pentameric complex.

Could these motions be related to the translation cycle on the ribosome? The rate of synthesis in prokaryotic ribosomes is about 10–20 amino acid residues per second [24], i.e. during polypeptide synthesis the characteristic time of global spatial movements of the ribosome is in the millisecond time scale. This fact invokes an idea that the 'flip-flop' transitions of the L7/L12 N-domains around the symmetry axis might be coupled with polypeptide synthesis. In the proposed model the 180° turns of the N-domains might induce curling and uncurling of the L7/L12 hinge region. As a result, the C-domains would be able to close up and go backwards to/from

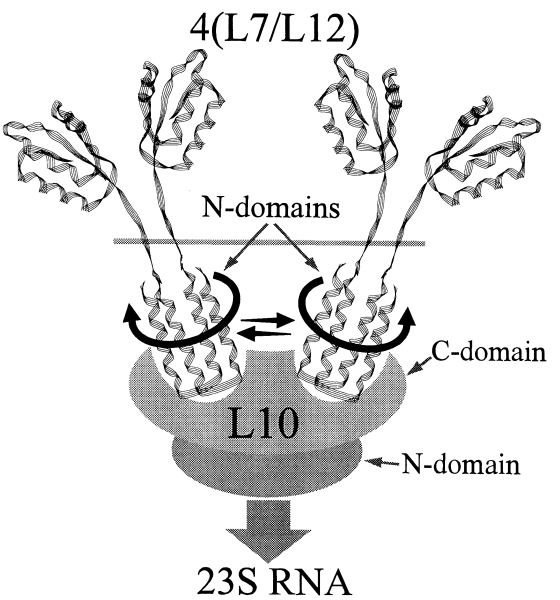

Fig. 3. Schematical representation of the interaction of two L7/L12 dimers with the L10 protein. Spatial structures of the L7/L12 dimers are presented as a ribbon diagram as in [3]. The horizontal line delimits NMR observable parts (residues Val^{40}–Lys^{120}) of the L7/L12 dimers. Suggested conformational motions of two symmetrical N-terminal helix bundles of the L7/L12 dimers are shown by black arrows.

the elongation factors bound to the ribosomal body. Rotation of the C-domains around the L7/L12 stalk axis cannot be excluded either. Consecutive interactions of the elongation factors with the ribosome, coupled with GTP hydrolysis, would order these movements during the translation process. The fact that L7/L12 C-domains interact with EF-G [6] and EF-Tu [25] bound to the ribosome is in favor of the hypothesis.

The role of symmetrical structure for the biological molecular rotary motor was recently demonstrated for mitochondrial F_1-ATPase [26]. We propose that a similar mechanism of 'rotational catalysis' might be involved in the interaction of the translation factors with the L7/L12 protein during protein synthesis.

Acknowledgements: The authors thank Dr. V.N. Bushuev for helpful discussions and Dr. L.I. Vasilieva for help in the preparation of the protein samples used. We also thank the Geneva University Hospital and the University of Geneva for the possibility of using the WWW molecular biology server ExPASy.

References

[1] Gudkov, A.T. (1997) FEBS Lett. 407, 253–256.
[2] Leijonmarck, M. and Liljas, A. (1987) J. Mol. Biol. 195, 555–580.
[3] Bocharov, E.V., Gudkov, A.T. and Arseniev, A.S. (1996) FEBS Lett. 379, 291–294.
[4] Gudkov, A.T., Budovskaya, E.V. and Sherstobaeva, N.M. (1995) FEBS Lett. 367, 280–282.
[5] Gudkov, A.T. and Behlke, J. (1978) Eur. J. Biochem. 90, 309–312.
[6] Bushuev, V.N. and Gudkov, A.T. (1988) Methods Enzymol. 164, 148–158.
[7] Hamman, B.D., Oleinikov, A.V., Jokhadze, G.G., Traut, R.R. and Jameson, D.M. (1996) Biochemistry 35, 16672–16679.
[8] Hamman, B.D., Oleinikov, A.V., Jokhadze, G.G., Traut, R.R. and Jameson, D.M. (1996) Biochemistry 35, 16680–16686.
[9] Bubunenko, M.G., Chuikov, S.V. and Gudkov, A.T. (1992) FEBS Lett. 313, 232–234.
[10] Gudkov, A.T., Tumanova, L.G., Venyaminov, S.Yu. and Khechinashvili, N.N. (1978) FEBS Lett. 93, 215–218.
[11] Möller, W., Groene, A., Terhorst, C. and Amons, R. (1972) Eur. J. Biochem. 25, 5–12.
[12] Liljas, A. (1982) Prog. Biophys. Mol. Biol. 40, 253–279.
[13] Bax, A. and Davis, D.G. (1985) J. Magn. Reson. 65, 355–366.
[14] Jeener, J., Meier, G.H., Bachman, P. and Ernst, R.R. (1979) J. tpdel 50
Chem. Phys. 71, 4546–4553.
[15] Wüthrich, K. (1986) NMR of Proteins and Nucleic Acids, Wiley, New York.
[16] Bax, A., Mitsuhiko, I., Kay, L.E., Torchia, D.A. and Tschudin, R. (1990) J. Magn. Reson. 86, 304–318.
[17] Zhang, O., Kay, L.E., Olivier, J.P. and Forman-Kay, J.D. (1994) J. Biomol. NMR 4, 845–858.
[18] Eccles, C., Xia, T.H., Billeter, M. and Wuthrich, K. (1991) J. Biomol. NMR 1, 111–130.
[19] Appel, R.D., Bairoch, A. and Hochstrasser, D.F. (1994) Trends Biochem. Sci. 19, 258–260.
[20] Wishart, D.S., Sykes, B.D. and Richards, F.M. (1991) J. Mol. Biol. 222, 311–333.
[21] Gudkov, A.T., Tumanova, L.G., Gongadze, G.M. and Bushuev, V.N. (1980) FEBS Lett. 109, 34–38.
[22] Liljas, A. and Garber, M. (1995) Curr. Opin. Struct. Biol. 5, 721–727.
[23] Oubridge, C., Ito, N., Evans, P.R., Teo, C.H. and Nagai, K. (1994) Nature 372, 432–438.
[24] Spirin, A.S. (1986) Ribosome Structure and Protein Biosynthesis, Benjamin/Cummings, Menlo Park, CA.
[25] Stark, H., Rodnina, M.V., Rinke-Appel, J., Brimacombe, R., Wintermeyer, W. and van Heel, M. (1997) Nature 389, 403–406.
[26] Noji, H., Yasuda, R., Yoshida, M. and Kinosita Jr., K. (1997) Nature 386, 299–302.